

# Motion of condensates in non-Markovian zero-range dynamics

Ori Hirschberg<sup>1</sup>, David Mukamel<sup>1</sup>, Gunter M. Schütz<sup>2</sup>

<sup>1</sup> Department of Physics of Complex Systems, Weizmann Institute of Science, Rehovot 76100, Israel

<sup>2</sup> Theoretical Soft Matter and Biophysics, Institute of Complex Systems, Forschungszentrum Jülich, 52425 Jülich, Germany

E-mail: ori.hirschberg@weizmann.ac.il, david.mukamel@weizmann.ac.il, g.schuetz@fz-juelich.de

**Abstract.** Condensation transition in a non-Markovian zero-range process is studied in one and higher dimensions. In the mean-field approximation, corresponding to infinite range hopping, the model exhibits condensation with a stationary condensate, as in the Markovian case, but with a modified phase diagram. In the case of nearest-neighbor hopping, the condensate is found to drift by a “slinky” motion from one site to the next. The mechanism of the drift is explored numerically in detail. A modified model with nearest-neighbor hopping which allows exact calculation of the steady state is introduced. The steady state of this model is found to be a product measure, and the condensate is stationary.

## 1. Introduction

In recent years, much progress has been made in the theoretical understanding of nonequilibrium condensation [1–3]. Condensation phenomena of this type are known to occur in a large variety of systems, where a macroscopic fraction of a conserved “mass” is accumulated in a microscopic portion of an extended system. Some examples of such systems are compartmentalized shaken granular gases [4], gelation, i.e., the formation of a macroscopic hub in complex network [5], condensation of wealth in economics [6], and the formation of traffic jams on highways [7].

An elucidation of the mechanism which lies behind the condensation transition in such systems was achieved by studying simplified but prototypical toy models, most notably the zero-range process (ZRP). In this process, particles hop stochastically between boxes with hopping rates which depend only on the occupation of the box from which each particle departs. This models diffusing particles which “interact” only with particles at the same location (i.e., the same box), and hence the name of the process. For any choice of hopping rates, the steady-state distribution of particles is known to factorize into single box terms and thus it may be computed exactly. Using

the exact solution, it was shown in [8] that a condensation transition may occur when the rate of hopping out of a box decreases with its occupation (modeling an attractive “interaction”). In this condensation transition, the system is homogeneous at small particle densities, while when the density exceeds a critical value, a single (randomly chosen) site is occupied by a macroscopic fraction of all particles.

When studying systems which exhibit a condensation transition, such as those listed above, the ZRP may be used to gain qualitative, and sometimes also quantitative, insight. This is done by mapping the dynamics of the system under consideration, usually in an approximate way, to that of the ZRP, and then utilizing known results for the ZRP [9–13]. Such a mapping is achieved by disregarding some of the structure of the original system, so that it can be reduced to the simplified balls and boxes picture of the ZRP. Underlying this procedure is an assumption that the condensation transition in the ZRP is universal in some sense, i.e., that the details which are lost when mapping a system to the ZRP are irrelevant to condensation.

This universality assumption was recently examined by studying how disregarding dynamical degrees of freedom may affect the condensation transition [14]. There, a small variation of the ZRP, which introduces temporal correlations in its dynamics, was found to have two main effects on the condensation transition: (i) a calculation in a mean-field setting showed that the non-Markovian nature of the dynamics “renormalizes” the parameters and critical exponents of the ZRP, and (ii) a numerical study of the model on a one-dimensional ring revealed that the temporally-correlated dynamics induces a “slinky” motion of the condensate throughout the system, whereby the condensate spills over from one site to the next. Thus, the nature of the condensed phase is modified in a qualitative manner.

In this paper we present a detailed analysis of the model introduced in [14]. First, we elaborate on the mean-field solution which was presented in [14] and generalize the results to a much broader class of hopping rates. We then turn to dynamics on a ring with hopping to the nearest-neighbor site and present a detailed study of the mechanism for the condensate drift. In studying the behavior of finite rings (of size  $L \leq 2000$  sites), we identify two different modes of condensate motion: motion through a barrier, in which the condensate is carried by a single site and spilling to the next site is initiated only once it overcomes a barrier, and motion with no barrier, in which the condensate is in a continual motion.

In addition, we consider a somewhat modified non-Markovian dynamics which allows an exact computation of the steady state on lattices of any dimension, even in the case of nearest-neighbor hopping. For this variant of the model we show that the steady-state distribution is given by a product measure, like in the Markovian ZRP, even though the currents of particles are temporally correlated. The exact solution of the model is shown to be qualitatively similar to the mean-field calculation, and in particular there is no condensate drift.

The paper is organized as follows. After describing the non-Markovian ZRP in Sec. 2, we present in Sec. 3 the full mean-field solution of the model and study how

condensation is affected by the non-Markovian dynamics. The numerical study of the condensation transition on a lattice with nearest-neighbor hopping is presented in Sec. 4. There we examine a particular choice of rates, which we term the on-off model, on a symmetric, totally asymmetric and partially asymmetric dynamics, and we analyze the mechanism for the motion of the condensate. In Sec. 5, we present the exactly solvable variant of the non-Markovian ZRP, calculate its steady state distribution and discuss condensation in this model.

## 2. Description of the model

We consider a system of  $N$  particles hopping between  $L$  boxes (labeled by  $i = 1, \dots, L$ ) with a mean density  $\rho = N/L$ . We are mainly interested in the thermodynamic limit in which  $L, N \rightarrow \infty$  with the density  $\rho$  kept constant. The state of each box is given by two variables: the number of particles in the box  $n_i$ , and a “clock” variable  $\tau_i$ . Both variables take non-negative integer values:  $n_i, \tau_i = 0, 1, 2, \dots$ . A configuration of the system is thus given by the set of pairs  $(\mathbf{n}, \boldsymbol{\tau}) = \{(n_i, \tau_i)\}_{i=1}^L$ .

The dynamics proceeds by particles jumping one at a time between the boxes, and, in parallel, by advances of the clocks. Conforming with the “zero-range” character of the ZRP, the rate with which a particle leaves a box is taken to depend only on the state of the box, i.e., on its occupation and clock state. We denote these hopping rates by  $u(n, \tau)$ . The clock dynamics is correlated with particle jumps: every time a particle jumps into a box, its clock is reset to zero. Independently, the clocks are advanced with a constant probability per unit time  $c$ . The two types of dynamical moves (a jump of a particle between two boxes  $i$  and  $j$ , and an advance of the clock at site  $i$ ) can be written as

$$\begin{aligned} (n_i, \tau_i), (n_j, \tau_j) &\xrightarrow{p_{ij}u(n_i, \tau_i)} (n_i - 1, \tau_i), (n_j + 1, \tau_j = 0) \\ (n_i, \tau_i) &\xrightarrow{c} (n_i, \tau_i + 1). \end{aligned} \quad (1)$$

Here,  $p_{ij}$  is a connectivity matrix which states the probability that a particle departing from site  $i$  will choose site  $j$  as its target. Particular choices of  $p_{ij}$  are further discussed below. The jump rates must satisfy  $u(0, \tau) = 0$  for all  $\tau$ , as a particle cannot jump out of an empty box.

To be precise about the meaning of “rate” this dynamics can be rephrased as follows: each box  $i$  of the lattice carries two alarm-clocks which ring after some random time. All  $2L$  alarm-clocks ring independently. Given that the state at box  $i$  is  $(n_i, \tau_i)$ , alarm-clock number 1 of this site rings after an exponentially distributed random time with parameter  $u(n, \tau)$ , while alarm-clock number 2 rings after an exponentially distributed random time with parameter  $c$ . If clock 1 rings first, a particle selects a target box  $j$  with probability  $p_{ij}$  and jumps to it. If clock 2 rings first, the internal clock at box  $i$  is incremented by one unit. After any change of the state at box  $i$ , the clocks ring again after an exponentially distributed random time determined by the updated state at box  $i$ .

The dynamical rules (1) are written for a general connectivity matrix  $p_{ij}$ . In this paper we concentrate mainly on two schemes for the choice of target box: mean-field (MF) dynamics, and a one-dimensional homogeneous ring geometry with nearest-neighbor hopping. In mean-field (MF) dynamics, the target box  $j \neq i$  is chosen randomly and uniformly from all boxes, i.e.,

$$p_{ij} = \frac{1}{L-1} \quad \text{for all } j \neq i. \quad (2)$$

In the case of ring dynamics, on the other hand, particles hop only between nearest-neighbor sites, possibly in an asymmetric fashion. Accordingly, the target box is chosen to be  $i+1$  with probability  $1-p$  and  $i-1$  with probability  $p$  (where box  $L+1$  is identified with box 1), i.e.,

$$p_{ij} = \begin{cases} (1-p) & (\text{if } j = i+1) \\ p & (\text{if } j = i-1) \\ 0 & \text{otherwise} \end{cases}. \quad (3)$$

Here,  $0 \leq p \leq 1$  is the asymmetry parameter: when it is equal to 0 the hopping is totally asymmetric and no hopping backwards can occur, while when  $p = 1/2$  the dynamics is completely symmetric. Below, MF dynamics is studied in Sec. 3, while ring dynamics is studied in Sections 4 and 5. We also briefly examine (in Sections 4.2.3 and 5.2) dynamics on higher-dimensional lattices. The generalization of (3) to the higher-dimensional case is rather straightforward and will be presented below when it is discussed.

The dependence of the jump rates on  $\tau$  renders the particle jump process, when it is taken by itself, non-Markovian, as the rate of a jump depends on how much time has passed since a particle hopped into the jump site. When considered in the higher dimensional space of occupations together with clocks, the full jump/increment process defined above is Markovian. Nevertheless, we will refer to this process as the non-Markovian ZRP, to stress the history dependence of the jump process.

The process may be implemented by a discrete-time Monte-Carlo version of this dynamics with random sequential update which is defined as follows: define  $p_{\max} = \max_{n,\tau}[u(n,\tau) + c]$ . For the Monte-Carlo update pick a random box uniformly and attempt to make one of the following changes: (i) move a particle to a target box (selected according to the appropriate scheme) with probability  $u(n,\tau)/p_{\max}$ , (ii) increment the internal clock with probability  $c/p_{\max}$ . A total of  $Lp_{\max}$  consecutive update attempts constitute one Monte-Carlo time unit.

A final remark on the nature of the clock variables. As is clear from the dynamical rules, the clock variables proceed in an irregular, stochastic fashion. Therefore, they do not measure the exact time that has passed since a particle last entered each site. Choosing clock variables which really measure time, i.e., which are continuous and proceed regularly, might seem more natural for some physical applications. Such regular clocks are not considered below, but we remark that they may be achieved starting from the dynamics (1) by taking an appropriate limit. This procedure is described in Appendix A.

### 3. The non-Markovian ZRP with mean-field dynamics

#### 3.1. General observations

In this section we analyze the non-Markovian ZRP with mean-field dynamics. In particular, we investigate how condensation is affected by the non-Markovian nature of the jump process.

Since each jump of a particle is to an arbitrarily chosen box, the MF dynamics does not generate correlations between different boxes beyond the correlations which arise from conservation of particles. Therefore, in the thermodynamic limit, the stationary distribution is expected to factorize into a product of single-box terms

$$\mathcal{P}(\mathbf{n}, \boldsymbol{\tau}) = Z_{L,N}^{-1} \prod_{i=1}^L P(n_i, \tau_i) \delta\left(\sum_{i=1}^L n_i - N\right), \quad (4)$$

where  $P(n_i, \tau_i)$  are the single-box occupation and clock probabilities, and the  $\delta$  function is a consequence of the conservation of particles. The normalization is given by

$$Z_{L,N} = \sum_{\mathbf{n}, \boldsymbol{\tau}} \prod_{i=1}^L P(n_i, \tau_i) \delta\left(\sum_{i=1}^L n_i - N\right). \quad (5)$$

As with the Markovian ZRP, the factorized stationary distribution provides the means for an analytic treatment of the model. In the thermodynamic limit, the single-box probabilities in the steady state  $P(n, \tau)$  are equal to those of a single box with a ‘‘mean-field’’ incoming current  $J$  which is generated by all other sites. The master-equation for the single site-box probability is

$$\frac{dP(n, \tau)}{dt} = JP(n-1)\delta_{\tau,0} + cP(n, \tau-1) + u(n+1, \tau)P(n+1, \tau) - P(n, \tau)[J + c + u(n, \tau)], \quad (6)$$

where the marginal occupation distribution is defined by  $P(n) \equiv \sum_{\tau} P(n, \tau)$ . The first term on the RHS corresponds to the box reaching the state  $(n, \tau = 0)$  by a particle entering a box with  $n - 1$  particles, the second to an advance of the clock into state  $\tau$ , the third to a particle leaving a box with  $n + 1$  particles, and the last to these three processes occurring when the box is in state  $(n, \tau)$ . This equation is also valid for  $n = 0$  or  $\tau = 0$  if one defines  $P(-1, \tau) = P(n, -1) = 0$  (and, as stated above,  $u(0, \tau) = 0$  must also hold). Once Eq. (6) is solved for a given MF current  $J$ , the current and the probability distribution are obtained by the self-consistency requirement

$$J = \sum_{n, \tau} u(n, \tau)P(n, \tau). \quad (7)$$

In the steady state,  $dP(n, \tau)/dt = 0$  and the master equation (6) yields

$$P(n, \tau)[J + c + u(n, \tau)] = JP(n-1)\delta_{\tau,0} + cP(n, \tau-1) + u(n+1, \tau)P(n+1, \tau). \quad (8)$$

Summing over all values of  $\tau$ , the terms containing  $c$  drop out telescopically, and one is left with the recursion relation

$$\bar{u}(n)P(n) = JP(n-1) \quad (9)$$

Here  $\bar{u}(n)$  is the mean hopping rate out of a site with  $n$  particles

$$\bar{u}(n) \equiv \frac{\sum_{\tau} P(n, \tau) u(n, \tau)}{\sum_{\tau} P(n, \tau)}. \quad (10)$$

Equation (9) expresses the balance between the probabilities to jump into and out of a box with  $n$  particles. Iterating relations (9) yields, as in the Markovian ZRP, the steady-state occupation probability

$$P(n) = P(0) J^n \bar{f}(n), \quad (11)$$

where the single-site weights are given by

$$\bar{f}(n) = \prod_{k=1}^n \bar{u}(k)^{-1}, \quad (12)$$

and  $P(0)^{-1} = 1 + \sum_{n=1}^{\infty} J^n \bar{f}(n)$  ensures the proper normalization of  $P(n)$ . The marginal distribution (11) and (12) is the same distribution one obtains for a Markovian ZRP but with the jump rates  $u(n)$  replaced by the effective rate  $\bar{u}(n)$  [1, 15].

Since the stationary distribution of our model has a similar form to that of a Markovian ZRP, the analysis of condensation in the model may also proceed in a similar fashion. We therefore briefly review how condensation takes place in the Markovian ZRP [1]. The occurrence of condensation in the Markovian ZRP is determined by the asymptotic behavior of the jump rates  $u(n)$  for large  $n$ . Two types of condensation may be distinguished: strong condensation, which occurs when the hopping rates tend to zero for large  $n$ , and weak condensation, which may occur when the hopping rates decrease to a constant value. In condensation of the strong type all particles accumulate in one box and the current vanishes in the thermodynamic limit. This condensation occurs at all densities (i.e., the critical density for condensation is  $\rho_c = 0$ ). Weak condensation takes place only when the rates decrease to a constant more slowly than  $1 + 2/n$ . In particular, when the rates have the form

$$u(n) = \gamma(1 + b/n^{\sigma} + o(1/n^{\sigma})) \quad (13)$$

for large  $n$ , condensation occurs above some critical density provided that  $\sigma < 1$  or  $\sigma = 1$  and  $b > 2$ . The critical density  $\rho_c$  is non-universal, i.e., it depends on the exact form of the rates  $u(n)$ . Importantly, the parameter  $\gamma$  only sets the time scale for the process and has no effect on the stationary distribution and the condensation transition.

In the weak condensation scenario, a single site (the condensate), chosen spontaneously at random, accommodates  $L(\rho - \rho_c)$  particles, while the density at all other sites remains  $\rho_c$ . The condensation transition is thus manifest in the occupation probability of a single site,  $P(n)$ . For the marginal case of  $\sigma = 1$ , the probability to find  $n$  particles in a given site decays exponentially as  $P(n) \sim n^{-b} e^{-n/\xi}$  for densities below the critical density, where  $\xi(\rho)$  diverges as  $\rho_c$  is approached. At the critical density, the occupation probability has a power law tail  $P(n) \sim n^{-b}$ . Above the critical density, the occupation of all background sites remains power-law distributed, while the occupation of the condensate is narrowly distributed around  $L(\rho - \rho_c)$  [16].

### 3.2. Condensation in an “on-off” model

As the effective jump rates  $\bar{u}(n)$  play the role of  $u(n)$  in the non-Markovian ZRP, it is their asymptotic behavior for  $n \rightarrow \infty$  which determines condensation in the model. The remainder of this section concentrates on the determination of this asymptotic behavior. We begin by discussing a simple choice of jump rates — an “on-off” model which will now be introduced — before turning to an analysis of more general jump rates.

We start the discussion by considering jump rates of the form

$$u(n, \tau) = \begin{cases} 0 & \tau = 0 \quad (\text{“off” state}) \\ u(n) & \tau \geq 1 \quad (\text{“on” state}). \end{cases} \quad (14)$$

In this case, every time a particle hops into a box, that box is turned “off”. When the box is in this off state no particle can leave it. After an exponentially distributed random time (with parameter  $c$ ) the box is turned back “on”, and particles can once more jump out of it with a rate  $u(n)$ . The model with these special rates will be called the *on-off model*.

In the on-off model, the dynamics depends only on whether  $\tau = 0$  or  $\tau \geq 1$ , and thus the clock has effectively only two states. Correspondingly, the state of a box can be characterized by  $P_{\text{off}}(n) \equiv P(n, \tau = 0)$  and  $P_{\text{on}}(n) = \sum_{\tau \geq 1} P(n, \tau)$ . The stationary master equation (8) is then given by

$$P_{\text{off}}(n)[J + c] = JP(n-1) \quad (15)$$

$$P_{\text{on}}(n)[J + u(n)] = cP_{\text{off}}(n) + P_{\text{on}}(n+1)u(n+1). \quad (16)$$

The solution of these equations is made simple, compared with a general non-Markovian ZRP, because the term  $p(n+1)u(n+1, 0)$  which should appear in the RHS of (15) (see Eq. (8)) vanishes.

To solve these equations we first note that by summing Eq. (15) over all values of  $n$  we find that the probability to find a site in the off state is

$$P_{\text{off}} \equiv \sum_n P_{\text{off}}(n) = \frac{J}{c+J}. \quad (17)$$

Next, an expression for  $P_{\text{off}}(n)$  is found from Eq. (15) together with (9) and (17),

$$P_{\text{off}}(n) = \frac{\bar{u}(n)P(n)}{J+c} = \frac{P_{\text{off}}}{J}\bar{u}(n)P(n). \quad (18)$$

A similar expression for  $P_{\text{on}}(n)$  is found by substituting the rates  $u(n, \tau)$  (which are of the form (14)) into Eq. (10), yielding

$$P_{\text{on}}(n) = \frac{\bar{u}(n)}{u(n)}P(n). \quad (19)$$

The effective jump rates  $\bar{u}(n)$  can now be obtained from (18) and (19) using  $P_{\text{off}}(n) + P_{\text{on}}(n) = P(n)$ , and are given by

$$\frac{1}{\bar{u}(n)} = \frac{P_{\text{off}}}{J} + \frac{1}{u(n)}. \quad (20)$$

This equation states that the mean time between hops from a site with  $n$  particles is equal to the mean time this site is in an “off” state plus the time it takes a particle to hop out once the system is already “on”.

Using Eqs. (11), (12), (17) and (20), it is now possible to obtain  $P(n)$  for any  $J$ , and subsequently the entire probability distribution is found via (18) and (19). Note that  $P(n)$  which is found this way depends on  $J$  both directly, as seen in Eq. (11), and indirectly through the effective rates (20). To finish the calculation, one must find the dependence of the current  $J$  on the density  $\rho$ . This can in principle be achieved by inverting the relation  $\rho(J) = \sum_n nP(n)$ . The effective hopping rates (20) are thus a function of the density.

To determine whether or not condensation may occur in the model, only the asymptotic form of  $\bar{u}(n)$  is needed. By examining Eq. (20) it is seen that  $\bar{u}(n)$  decreases to zero when  $n \rightarrow \infty$  if and only if  $u(n)$  decreases to zero, and similarly  $\bar{u}(n)$  decreases to a constant if and only if  $u(n)$  decreases to a constant. Therefore, strong condensation is not affected by the clock-dependent dynamics. To study weak condensation, assume jump rates of the asymptotic form (13) with  $\gamma = 1$  (as explained above,  $\gamma$  sets the time scale of the process, and can be set to 1 without loss of generality). From Eqs. (17) and (20) we find, to leading order in  $1/n$

$$\bar{u}(n) = \frac{c + J}{c + J + 1} \left( 1 + \frac{b_{\text{eff}}}{n^\sigma} + o\left(\frac{1}{n^\sigma}\right) \right), \quad (21)$$

which is again of the form (13) but with an effective hopping parameter

$$b_{\text{eff}} = \frac{c + J}{c + J + 1} b < b. \quad (22)$$

If  $\sigma < 1$  condensation occurs in the on-off model as it does in the Markovian ZRP. In the commonly encountered case of  $\sigma = 1$ , however, condensation only occurs when  $b_{\text{eff}} > 2$ . The critical current at the condensation transition is given in this case by  $J_c = \lim_{n \rightarrow \infty} \bar{u}(n)$  [1], which yields, according to (21),  $J_c = (c + J_c)/(c + J_c + 1)$ , or

$$J_c = \frac{c}{2} \left( \sqrt{1 + \frac{4}{c}} - 1 \right). \quad (23)$$

This allows us to write

$$b_{\text{eff}} = J_c b. \quad (24)$$

Therefore, condensation takes place when the hopping parameter satisfies  $b > \frac{4}{c} \left( \sqrt{1 + 4/c} - 1 \right)^{-1}$ . The critical value of  $b$  is larger than 2, in contrast with the Markovian case for which the critical value for condensation is  $b = 2$ .

### 3.3. Condensation in MF models with more general rates

In the previous section we have seen that in the case of jump rates with an asymptotic form

$$u(n) = 1 + b/n + \dots, \quad (25)$$



the on-off dynamics leads to an effective value of  $b$ , and thus it may affect the occurrence of the condensation transition. We now demonstrate that this holds also when the clock dependence is more general than the on-off case, and we show how  $b_{\text{eff}}$  may be calculated. To this end we consider rates of the form

$$u(n, \tau) = u(n)v(\tau) = \left(1 + \frac{b}{n} + \dots\right)v(\tau) \quad (26)$$

where  $u(n)$  has been taken to be of the form (25).

As mentioned above, the stationary master equation (8) is harder to analyze when the rates are not of the on-off type, because  $P(n, \tau)$  depends in (8) on  $P(n, \tau + 1)$ . However, since only the large  $n$  asymptotics of  $\bar{u}(n)$  and  $P(n, \tau)$  at criticality affect condensation, it is possible to make progress by restricting the discussion to these quantities. We therefore assume that  $J = J_c$  and make the following ansatz:

$$\begin{aligned} \bar{u}(n) &= J_c \left[1 + \frac{b_{\text{eff}}}{n} + o\left(\frac{1}{n}\right)\right] \\ P(n, \tau) &= An^{-b_{\text{eff}}} \alpha(\tau) \left[1 + \frac{d(\tau)}{n} + o\left(\frac{1}{n}\right)\right] \\ P(n) &= An^{-b_{\text{eff}}} \left[1 + \frac{d}{n} + o\left(\frac{1}{n}\right)\right]. \end{aligned} \quad (27)$$

This ansatz is motivated by the solution of the on-off model (compare with Eqs. (18) and (21)). The constant  $A$  is a normalization constant, and from the definition  $P(n) = \sum_{\tau} P(n, \tau)$  it is seen that  $\sum_{\tau} \alpha(\tau) = 1$  and  $\sum_{\tau} \alpha(\tau)d(\tau) = d$  must hold.

Substituting the ansatz (27) in the stationary master equation (8) and equating terms order by order in  $1/n$  yields to order  $O(1)$

$$\alpha(\tau) = \frac{J_c}{J_c + c} \left(\frac{c}{J_c + c}\right)^{\tau} \quad (28)$$

and to order  $O(1/n)$

$$d(\tau) = d - \left[\frac{1}{J_c + c} \sum_{\tau'=0}^{\tau} v(\tau') - 1\right] b_{\text{eff}}. \quad (29)$$

The current and  $b_{\text{eff}}$  can now be found by substituting (27) in the definition of  $\bar{u}(n)$  (Eq. (10)) and equating once again order by order in  $1/n$ . To order  $O(1)$ , an equation for the critical current is obtained

$$J_c = \sum_{\tau=0}^{\infty} \alpha(\tau)v(\tau) = \frac{J_c}{J_c + c} \sum_{\tau=0}^{\infty} \left(\frac{c}{J_c + c}\right)^{\tau} v(\tau), \quad (30)$$

where (28) was used in the last equality. To order  $O(1/n)$ , using (28) and (29),  $b_{\text{eff}}$  is found to satisfy

$$\begin{aligned} b_{\text{eff}} &= J_c(J_c + c) \left[ \sum_{\tau=0}^{\infty} \sum_{\tau'=0}^{\tau} \alpha(\tau)v(\tau)v(\tau') \right]^{-1} \cdot b \\ &= (J_c + c)^2 \left[ \sum_{\tau=0}^{\infty} \sum_{\tau'=0}^{\tau} \left(\frac{c}{J_c + c}\right)^{\tau} v(\tau)v(\tau') \right]^{-1} \cdot b \end{aligned} \quad (31)$$

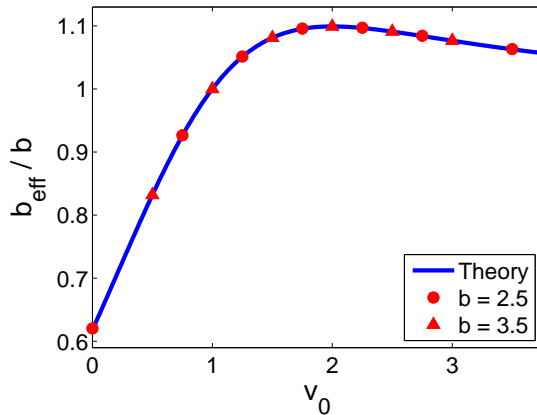


Figure 1: The mean-field value of  $b_{\text{eff}}/b$  as a function of  $v_0$  for the rates (32). The line corresponds to the prediction (31), while the symbols were obtained by numerically integrating the mean-field master equation (6) with  $J = J_c$  of (30). Note that  $b_{\text{eff}}$  may be either smaller or larger than  $b$ , depending on  $v_0$ .

The calculation outlined above is valid as long as the series in (30) and (31) converge. The exponential form of  $\alpha(\tau)$  in Eq. (28) implies that convergence is guaranteed if  $v(\tau)$  decays or grows slower than exponentially. In particular, this implies that the results are correct if  $v(\tau)$  tends to a finite (non-zero) constant for large  $\tau$ . Note that if  $v(\tau)$  decays to zero fast enough, although the series converge any system of a finite size will eventually be frozen in an absorbing state in which all  $\tau$ 's tend to infinity and no particles jump.

Equation (31) implies that, as found in the particular case of the on-off model, the condensation behavior depends on the memory effects induced by the clocks. Note, however, that unlike the on-off case,  $b_{\text{eff}}$  is not necessarily smaller than  $b$ . For instance, consider rates of the form (26) with

$$v(\tau) = \begin{cases} v_0 & \tau = 0 \\ 1 & \tau \geq 1 \end{cases}. \quad (32)$$

For  $v_0 = 0$  these rates reduce to the on-off model, while  $v_0 = 1$  is the Markovian ZRP. For arbitrary  $v_0$ , Eq. (30) yields  $J_c = (v_0 - c + \sqrt{(v_0 - c)^2 + 4c})/2$ , and Eq. (31) yields  $b_{\text{eff}} = b(c + v_0 J_c)/(c + v_0 J_c + J_c - v_0)$ . This result, which is plotted in Fig. 1, demonstrates that for different values of  $v_0$  and  $c$ , the effective hopping parameter  $b_{\text{eff}}$  might be larger or smaller than the “bare” value  $b$ .

#### 4. The non-Markovian ZRP with nearest-neighbor dynamics

The results of the previous section demonstrate that temporal correlations in the dynamics of a mean-field ZRP affect the condensation transition. In this section we examine whether this mean-field picture persists also when the dynamics allows only nearest-neighbor hopping, and whether new effects appear in the latter case.

In the on-off model with nearest-neighbor hopping dynamics, the stationary distribution does not factorize and the stationary solution of the Master equation is not known. We therefore study the model using numerical Monte-Carlo simulations. From these simulations we find that condensation does indeed seem to be controlled by an effective hopping parameter  $b_{\text{eff}}$ , albeit with a value which differs from the MF prediction. We also find that asymmetric jump rates may cause the condensate to drift with a finite velocity.

In this section we concentrate solely on the on-off model with jump rates of the form (14) and (25), unless explicitly stated otherwise.

#### 4.1. On-off model with symmetric nearest-neighbor hopping

We begin the discussion of a ring with nearest-neighbor hopping dynamics by considering an on-off model with symmetric hopping, i.e., with  $p = 1/2$ . Note that, unlike the Markovian ZRP with symmetric hopping, which satisfies detailed balance and hence is an equilibrium model, the non-Markovian ZRP does not satisfy detailed balance even when it is symmetric. To understand why, note that there are allowed dynamical moves whose reverse cannot occur (such as an advance of a clock, or a jump of a particle simultaneously with resetting the clock of the target site to zero). As these moves have a non-zero probability to occur in the steady state, stationary probability currents must exist.

Monte-Carlo simulations of the on-off model with nearest neighbor hopping were carried out on a ring of size  $L = 500$  boxes with different particle densities and  $b = 4.5$ . The system was initialized to a state in which all particles were located at the first site and all sites were “on”, and the dynamics was run for a time of  $t_{\text{equil}} = 2.5 \cdot 10^7$  time units to allow the system to reach a steady state. After this equilibration time, the state of the system was recorded every  $t_{\text{sampling}} = 5000$  time units. The measured single site occupation probability  $P(n)$  and typical snapshots of the lattice for different values of  $\rho$ , presented in Fig. 2, show a qualitative resemblance to those of a Markovian ZRP. At small densities when the system is in the fluid phase, the single site occupation probability has an exponential tail, while at high densities this probability develops a peak which corresponds to the condensate. The transition takes place at a critical density (which is found to be  $\rho_c \approx 2.75$ ) at which the occupation probability decays as a power law of the form  $P(n) \sim n^{-b_{\text{eff}}}$ . In finite systems this power law has an exponential cutoff due to finite size effects.

Measuring the effective hopping parameter  $b_{\text{eff}}$  numerically is a difficult task because it depends on the tail of the probability distribution which is strongly distorted by finite size effect. However, simulation results indicate that  $b_{\text{eff}}$  for symmetric hopping is larger than the MF value (24) and smaller than the “bare” value  $b$  (see Figure 2).

The simulation results indicate that the conclusions which were found for mean-field dynamics are qualitatively correct for symmetric nearest-neighbor dynamics.

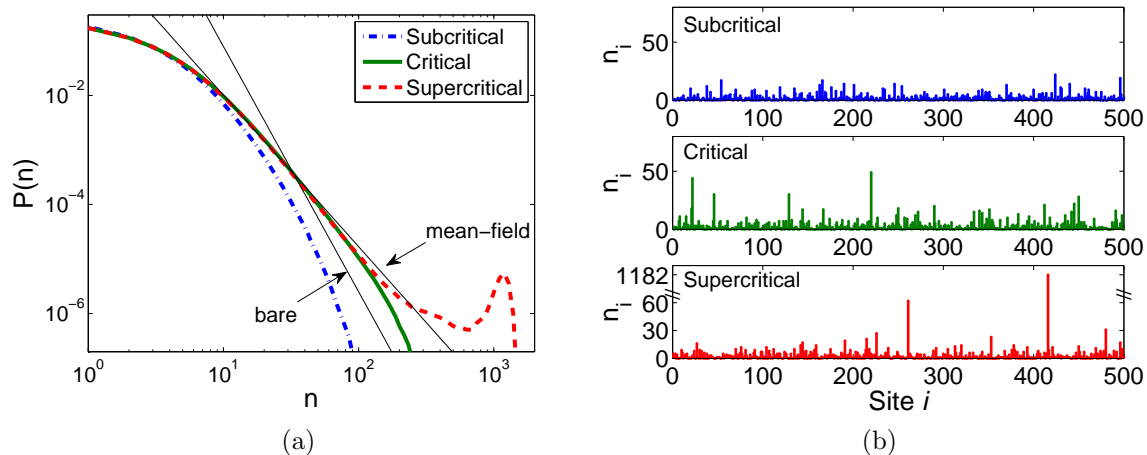


Figure 2: (a) The occupation probability  $P(n)$  of a single site in a ring with symmetric nearest-neighbor on-off dynamics for several densities. (b) Typical snapshots of the lattice for several densities. Results were obtained by Monte-Carlo simulations with  $b = 4.5$ ,  $c = 1$  and  $L = 500$  sites, for a subcritical density ( $\rho = 2$ ), a supercritical density ( $\rho = 5$ ) and at the critical region ( $\rho = 2.75$ ). The two thin straight line in (a) correspond to the power laws  $P(n) \sim n^{-b}$  and  $P(n) \sim n^{-b_{\text{eff}}}$  of the bare value  $b = 4.5$  and the mean-field effective value  $b_{\text{eff}} \approx 2.78$  of Eq. (24). The power-law exponent for symmetric dynamics is seen to lie between these two values. Note that in the supercritical case, the y-axis of figure (b) is broken in order to show both the condensate and the disordered background.

#### 4.2. On-off model with asymmetric nearest-neighbor hopping

Simulations of asymmetric nearest-neighbor dynamics (i.e., with  $p < 1/2$ ) indicate that, as with the symmetric case, condensation is controlled by an effective hopping parameter. However, a new effect is found in simulations of asymmetric hopping: the condensate drifts with a finite velocity. Two different drift regimes are observed in simulations of finite systems: a “strong drift” regime in which the condensate is in a continual motion, and a “weak drift” regime in which the condensate stays for some (random) time in each site before jumping to the next. In what follows we begin by discussing the case of totally asymmetric hopping dynamics, (i.e., with asymmetry parameter  $p = 0$ ), where we examine the strong drift and the weak drift regimes separately. We then discuss more general asymmetric dynamics, including partially asymmetric hopping and asymmetric dynamics on higher dimensional lattices.

*4.2.1. Totally asymmetric hopping: strong drift regime* Monte-Carlo simulations of a ring with totally asymmetric nearest-neighbor on-off hopping dynamics were carried out for different values of  $c$ . The results of these simulations show that for small values of  $c$  the condensate drifts continuously in what we term a strong drift regime. In this

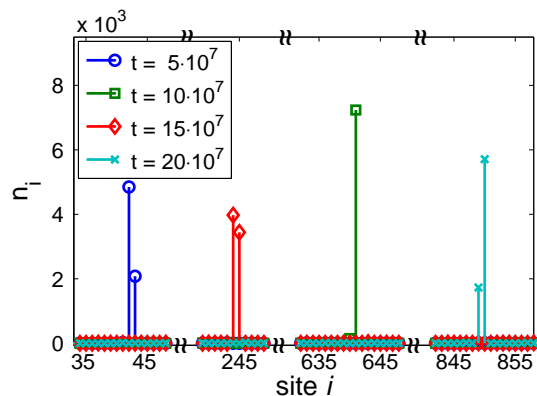


Figure 3: Snapshots of the on-off model with totally-asymmetric nearest-neighbor hopping on a ring, showing the occupation numbers  $n_i$  at and in the vicinity of the condensate at four points in time. Here,  $L = 1000$  sites,  $\rho = 10$ ,  $b = 5.5$ , and  $c = 1$ . The condensate occupies two sites and drifts with a constant mean velocity.

regime, the condensate typically occupies two adjacent boxes  $i$  and  $i + 1$ , in contrast to previously known condensation phenomena. In addition, The location of these two boxes advances with time. This is demonstrated in Fig. 3, where we present snapshots of the lattice taken at different times as obtained from a simulation with  $L = 1000$  boxes.

An inspection of the microscopic dynamics shows that the drift of the condensate takes place via a “slinky” motion in which the second condensate site,  $i + 1$ , accumulated particles at the expense of the first condensate site,  $i$ . This slinky motion results from the fact that site  $i + 1$  is turned off more often than other sites. In other words, the effective hopping rates out of a site are no longer homogeneous in space, but rather they depend on the distance of the site from the condensate, and in particular, the mean current out of the condensate is larger than the mean current out of the next site:  $\langle \bar{u}_i(n_i) \rangle > \langle \bar{u}_{i+1}(n_{i+1}) \rangle$ . Thus particles accumulate on site  $i + 1$  until site  $i$  is no longer macroscopically occupied, giving the clock at  $i + 1$  the chance to reach the on state for durations of time sufficiently long to allow particles to escape. Then particles start to hop from site  $i + 1$  to site  $i + 2$  in the same fashion and the slinky motion continues. This mechanism for condensate motion was recently found in other models, and will be analyzed in more detail elsewhere [17].

This slinky motion mechanism suggests that the drift velocity  $v_{\text{drift}}$  is inversely proportional to the number of particles in the condensate  $N_{\text{cond}}$ , i.e.,

$$v_{\text{drift}}^{-1} \sim N_{\text{cond}} = N - N_{\text{bg}} = L(\rho - \rho_{\text{bg}}), \quad (33)$$

where  $N_{\text{bg}} \equiv N - N_{\text{cond}}$  and  $\rho_{\text{bg}} \equiv N_{\text{bg}}/(L - 2)$  are respectively the mean number and the density of particles in the background fluid, i.e., in all sites but the condensate sites. In the thermodynamic limit, the velocity of the condensate vanishes. It should be noted that this drift motion of the condensate is different from the relocation of the condensate which occurs in Markovian ZRPs. In the Markovian case, a condensate on any finite

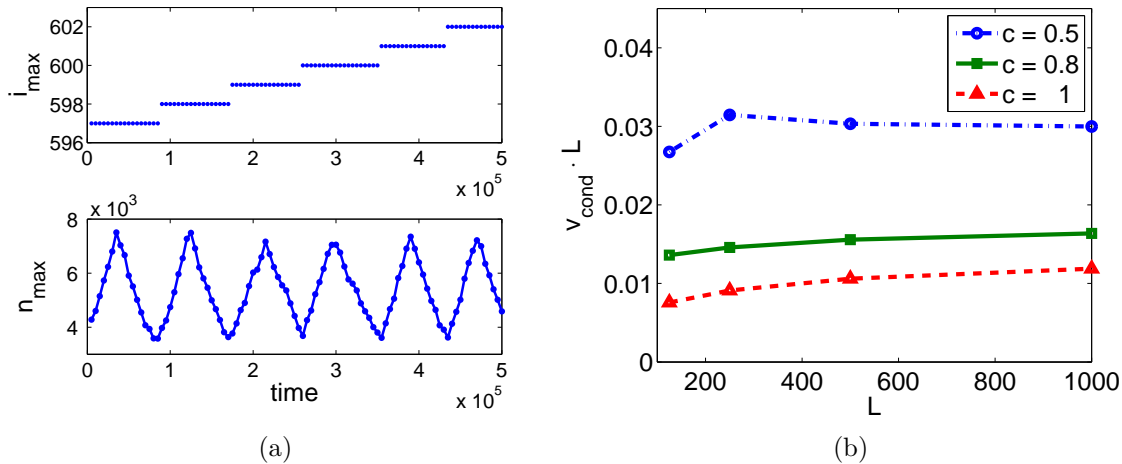


Figure 4: (a) The “slinky” motion of the condensate is seen in the position of the most occupied site  $i_{\max}$  and its occupation number  $n_{\max}$  as a function of time, on a ring of size  $L = 1000$  with  $c = 1$ . (b) This slinky motion suggests that the velocity of the condensate scales as  $L^{-1}$ , as is demonstrated for different values of  $c$ . Graphs were obtained from simulation of totally-asymmetric nearest-neighbor on-off dynamics with  $\rho = 10$  and  $b = 5.5$ .

system can melt and reappear at some other randomly chosen site of the lattice. This relocation of the condensate happens on a characteristic time which scales with the system size to a power larger than 2 [18–21]. A similar relocation of the condensate to a random distant site is seen to occur also in the asymmetric on-off ZRP, superimposed on the “slinky” drift motion.

The snapshots presented in Fig. 3 clearly demonstrate that the condensate occupies two adjacent sites with varying relative occupation, consistent with the slinky motion described above. In addition, the drift of the condensate is evident in the figure. In order to demonstrate the slinky motion in more detail, we present in Fig. 4a a plot showing the position of the most occupied site  $i_{\max}$  and its occupation number,  $n_{\max}$ , as a function of time. The occupation number  $n_{\max}$  oscillates in time with approximately constant frequency. Typically it decreases linearly until it reaches its minimal value, when  $i_{\max}$  increases by 1 and  $n_{\max}$  starts increasing. Fig. 4b displays the scaling of the condensate velocity with the system size  $L$ , which agrees with the estimate of Eq. (33).

In Fig. 5 we present the single-site occupation probability distribution  $P(n)$  for various densities and for various system sizes. At high densities the distribution exhibits a plateau which reflects the particle distribution among the two sites which constitute the condensate. This is in contrast with a Markovian ZRP and the symmetric on-off model where the condensate is supported by a single site, which results in a sharp peak in  $P(n)$  (compare with the inset and with Fig. 2a). The value of  $P(n)$  at the plateau in the non-Markovian case may be estimated for  $\rho$  above the critical density and large  $L$

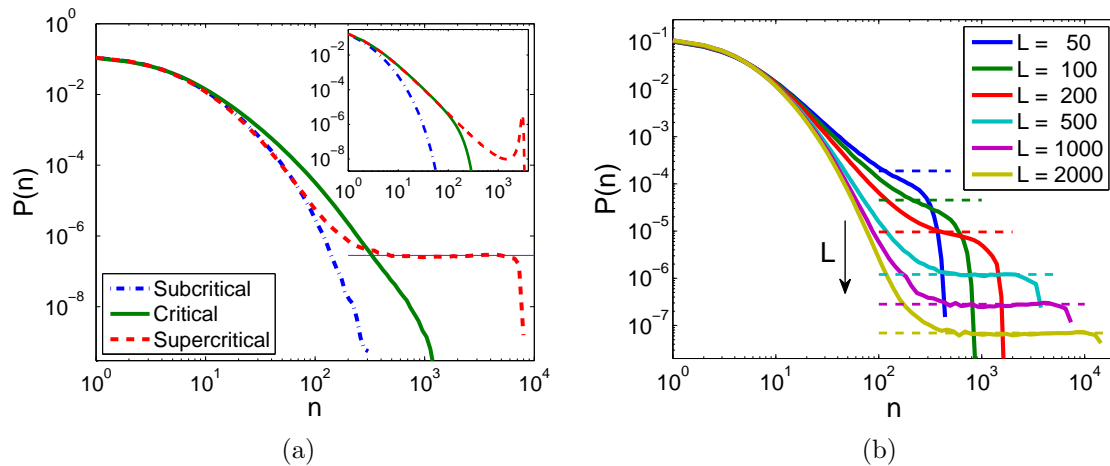


Figure 5: The occupation probability  $P(n)$  of a single-site in a ring with totally-asymmetric nearest-neighbor hopping and different densities, as obtained from Monte-Carlo simulations. (a)  $P(n)$  at a subcritical density ( $\rho = 3$ ), supercritical density ( $\rho = 10$ ) and at the critical region ( $\rho = 4.1$ ). The horizontal line indicates  $P_{\text{plateau}}$  of (34), where  $\rho_{\text{bg}}$  was obtained from the simulation. Here,  $L = 1000$ ,  $b = 5.5$  and  $c = 1$ . The inset shows for comparison a similar plot of  $P(n)$  for a Markovian ZRP of  $L = 1000$  sites with  $b = 3$ , in the subcritical ( $\rho = 0.5$ ) critical ( $\rho = 1$ ) and supercritical ( $\rho = 4$ ) phases. (b)  $P(n)$  for several system sizes ( $L$  increases in the direction of the arrow). The dashed horizontal lines indicates  $P_{\text{plateau}}$  of (34). Here  $\rho = 10$ ,  $b = 5.5$  and  $c = 1$ .

using the slinky motion of the condensate. The probability that a given site carries the condensate is  $2/L$ , and in such a site there is an approximately uniform probability to find any occupation  $0 < n < N_{\text{cond}} = L(\rho - \rho_{\text{bg}})$ . Thus,

$$P_{\text{plateau}} \sim \frac{2}{L} \frac{1}{L(\rho - \rho_{\text{bg}})}. \quad (34)$$

This estimate is in good agreement with the plateau value in Fig. 5. For small densities,  $P(n)$  decays exponentially, indicating the absence of a condensate. For the system size studied in this figure, the distribution at small values of  $n$  does not allow to extract a power law decay as expected for the condensation transition. At density  $\rho = 4.1$  there is a range of  $n$  for which  $P(n)$  seems to follow a power law with  $b_{\text{eff}} \approx 4$ . This value differs significantly from the bare parameter  $b = 5.5$ , the expected value for Markovian ZRP.

*4.2.2. Totally asymmetric hopping: weak drift regime* For larger values of the clock rate  $c$ , the motion of the condensate looks qualitatively different from that in the strong drift regime: the continuous slinky motion is replaced by an erratic slinky motion, in which the condensate spends a long period of time in each site before jumping to the next. We refer to this regime as the weak drift regime. This difference is observed on finite systems. Whether this type of motion persists for large  $L$  remains an open

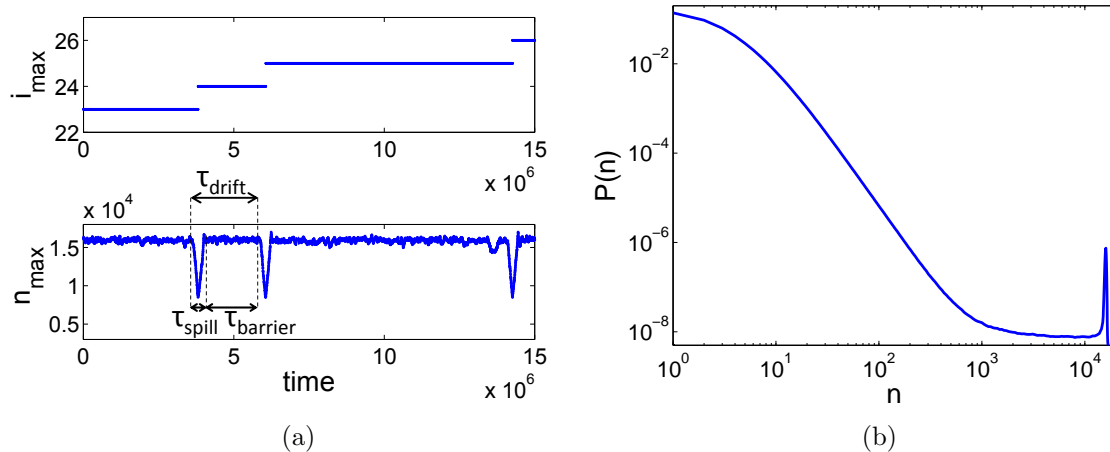


Figure 6: (a) The position of the most occupied site  $i_{\max}$  and its occupation number  $n_{\max}$  as a function of time, in the weak drift regime, as measured on a ring of size  $L = 2000$  with totally asymmetric hopping,  $b = 5.5$ ,  $\rho = 10$  and  $c = 2$ . The times  $\tau_{\text{drift}}$ ,  $\tau_{\text{spill}}$  and  $\tau_{\text{barrier}}$  are illustrated in the bottom panel. (b) The occupation probability  $P(n)$  of a single-site measured in the same system. A plateau is still observed, reflecting the slinky motion during transitions for one site to the next. However, unlike the strong drift regime, there is a peak at high densities reflecting the periods of time when the condensate is motionless.

question at this point, as there are some indications that the thermodynamic behavior might be similar to the strong drift motion in this limit. In what follows we present the numerical evidence for the weak drift regime, and provide details on the question of the thermodynamic limit.

All three main features which characterize the strong drift regime — a condensate that occupies two sites, its continual drift, and a plateau in the single site occupation probability — are modified in the weak drift regime. In this regime, the condensate occupies a single site for a long duration of time, and it occupies two sites only during the (relatively short) time of transition from one site to the next. This is clearly seen in Fig. 6a, where the occupation and location of the most occupied site are shown as a function time for a system of size  $L = 2000$  with  $c = 2$  and  $b = 5.5$  (compare with Fig. 4a, and note the difference in the scale of the time axes). As a result, a sharp peak is seen in the single site occupation probability at large values of  $n$  (Fig. 6b). A plateau is still found at intermediate values of  $n$ , but it no longer follows the scaling relation (34).

The characteristics of the weak drift described above suggest that the condensate is stabilized in one site by a “barrier”. The slinky motion is initiated only once fluctuations overcome this barrier and the number of particles in the condensate decreases beyond some threshold, or, alternatively, when the number of particles in the next site increases beyond a threshold.

A possible microscopic mechanism which would give rise to such a threshold is as



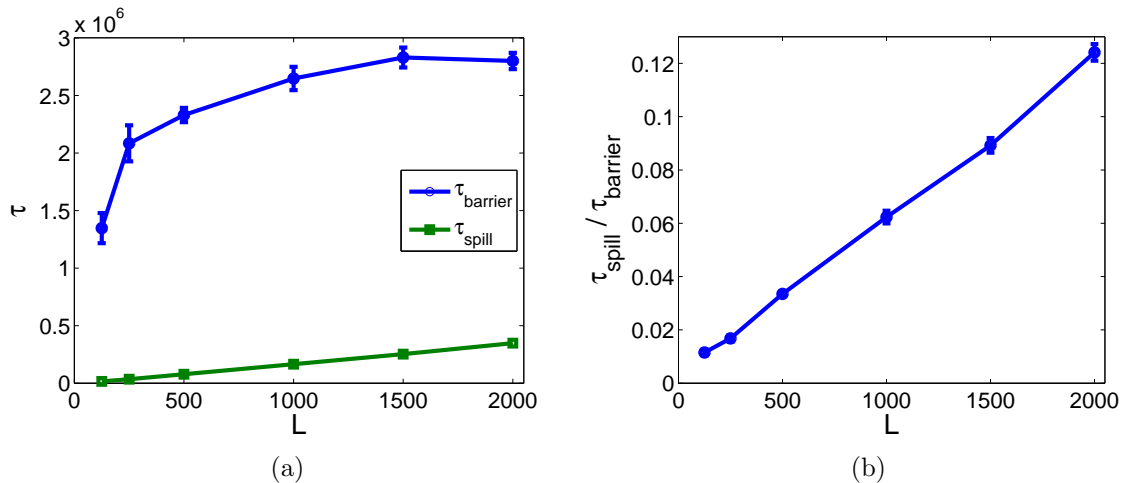


Figure 7: (a)  $\tau_{\text{barrier}}$  and  $\tau_{\text{spill}}$  (see Fig. 6a) as a function of the system size. (b) The ratio  $\tau_{\text{spill}}/\tau_{\text{barrier}}$  as a function of the system size. For the system sizes which we could simulate, the condensate motion has not yet converged to its thermodynamic limit behavior. If the trend shown here continues at larger  $L$ , eventual condensate motion will be similar to that seen in the strong drift regime. The parameters used in the simulation are the same as those of Fig. 6.

follows. Suppose the condensate is located at site 1. As discussed above, the drift motion of the condensate indicates that the mean current out of site 1 is greater than that leaving site 2, i.e.,  $\langle \bar{u}_1(n_1) \rangle > \langle \bar{u}_2(n_2) \rangle$ . However, if  $n_2$  is small enough, it might be that at some moment  $\langle \bar{u}_1(n_1) \rangle < \bar{u}_2(n_2)$ . In this case, because  $\bar{u}_i(n)$  is a decreasing function of  $n$ , particles begin to accumulate in site 2 only after its occupation exceeds a value  $n^*$  which is defined by  $\bar{u}_2(n^*) = \langle \bar{u}_1(n_1) \rangle$ . Thus, the condensate begins to spill from site 1 to 2 only after a random fluctuation brings the occupation of site 2 to  $n^*$ . If  $n^*$  is large enough, the time until such a fluctuation occurs can be long. However, this time is expected to remain finite in the thermodynamic limit  $L \rightarrow \infty$ . If this picture is correct, the erratic motion of the condensate which characterizes the weak drift regime is expected to be negligible in the thermodynamic limit, since the time of the spilling of the condensate scales as the system size  $L$ . A more detailed study of such a mechanism for a weak condensate drift will be presented elsewhere [17].

It is not yet known whether this picture provides an accurate description of the microscopic mechanism which leads to the weak drift motion. However, numerical evidence indicates that the weak drift regime may indeed exist only as a finite size effect. To address this question, we compare the typical time that the condensate resides on a single site, which we term  $\tau_{\text{barrier}}$ , with the time it takes the condensate to “spill” from one site to the next, which we denote  $\tau_{\text{spill}}$ . Together, these two time add up to give the typical time for the drift motion:  $\tau_{\text{drift}} \equiv v_{\text{drift}}^{-1} = \tau_{\text{spill}} + \tau_{\text{barrier}}$ , see Fig. 6a. In Fig. 7a, we present the dependence of  $\tau_{\text{barrier}}$  and  $\tau_{\text{spill}}$  on the system size. For the system sizes which we were able to study numerically,  $\tau_{\text{spill}}$  was seen to grow linearly with  $L$  as

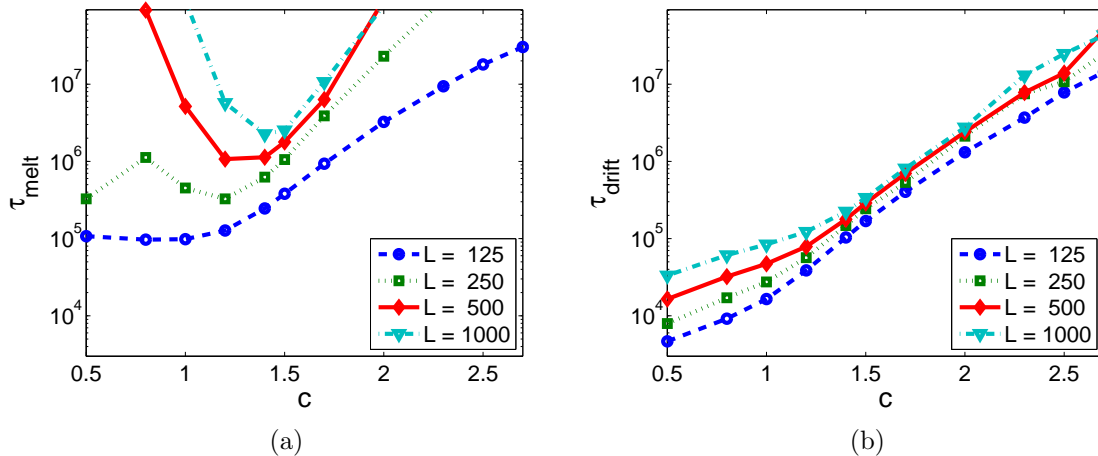


Figure 8: The mean time between (a) drift movements of the condensate ( $\tau_{\text{drift}}$ ) and (b) melting movements ( $\tau_{\text{melt}}$ ) as a function of  $c$  for several values of  $L$ . The entire duration of the simulation was  $\sim 10^9$  time units, and thus the plots are cut off at  $\tau \approx 10^8$ , beyond which the melting time can no longer be estimated reliably with the data available. The parameters of the simulation are the same as those of Fig. 6. Lines are guides to the eye.

expected (it should take twice as long to move twice as many particles from one site to the next). However,  $\tau_{\text{barrier}}$  is seen to grow slower than linearly. This trend, which is emphasized when looking at the ratio  $\tau_{\text{spill}}/\tau_{\text{barrier}}$  (see Fig. 7b) indicates that although  $\tau_{\text{spill}} \ll \tau_{\text{barrier}}$  for the system sizes which were studied, the situation might be reversed at large enough systems, in which case the motion of the condensate will be similar to that in the strong drift regime. Whether this trend continues at larger values of  $L$  remains an open question.

Numerical limitations also hindered the study of the behavior of the system at the transition between the strong and weak drift regimes, as well as at higher values of  $c$ . At values of  $1 < c < 2$ , there is a sharp decrease of the mean time  $\tau_{\text{melt}}$  between events at which the condensate melts and reappears in a distant site (see Fig. 8a). For the values of  $L$  which we were able to study these events were still quite frequent, indicating that the system was still far from thermodynamic behavior. As  $\tau_{\text{drift}}$  is seen to grow roughly exponentially with  $c$  (see Fig. 8b), when  $c$  is larger than about 2,  $\tau_{\text{drift}}$  becomes comparable with the total length of the simulation.

*4.2.3. Other types of asymmetric dynamics* The main features of the on-off model, and specifically the drift of the condensate which was discussed above for the case of totally-asymmetric hopping, are quite robust to small changes in the dynamics of the model. We shall now mention a few such modified models which exhibit a similar behavior in the condensed phase.

We begin with the on-off model with partially asymmetric dynamics, where each

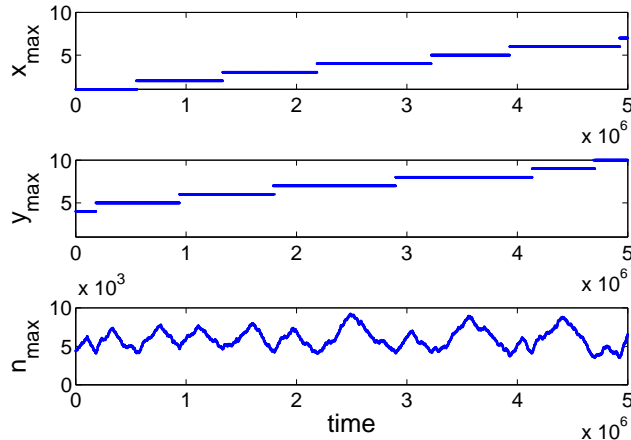


Figure 9: Drift of the condensate in a 2-dimensional square lattice with bias to the up and right directions. The top two panels show the  $x$ - and  $y$ -components  $x_{\max}$  and  $y_{\max}$  of the location of the most occupied site as a function of time and the bottom panel its occupation number  $n_{\max}$ . The lattice is of size  $20 \times 20$ , and the parameters of the simulation are  $\rho = 30$ ,  $b = 5.5$  and  $c = 0.4$ . The asymmetry of the hopping is as described in the text.

time a particle hops it can jump to the right with probability  $1 - p$  or to the left with probability  $p$ . Totally asymmetric dynamics corresponds to  $p = 0$ . If an asymmetric system is in the strong drift regime and  $p$  is increased slightly, no significant changes in its behavior are seen, and in particular it remains in the strong drift regime. When  $p$  is further increased, a transition to the weak drift regime occurs in the numerical simulations. This transition is similar to the one discussed above in the totally-asymmetric case when  $c$  is increased beyond 1, and it too is accompanied by a sharp dip in  $\tau_{\text{melt}}$ . For a system of size  $L = 1000$  with  $c = 1$  and  $b = 5.5$  the transition was found to occur at around  $p = 0.1$ . Beyond this transition, the drift velocity rapidly decreases as the dynamics approaches the symmetric dynamics at  $p = 1/2$  at which point no drift of the condensate is seen. It should be noted that in the symmetric case, when the condensate relocates to a different site there seems to be no preference to its neighboring sites. Rather, the condensate melts and reappears at a distant site, as in the Markovian case.

A drift of the condensate is also observed when the site is not turned completely off at  $\tau = 0$ . Simulations with hopping rates of the form  $u(n, \tau) = u(n)v(\tau)$  with  $v(\tau)$  as in Eq. (32),  $v_0 = 0.5$  and  $b = 5.5$ , exhibit strong drift behavior when  $c = 0.4$  and weak drift behavior when  $c = 1$ .

Condensate drift, both weak and strong, also occurs in 2-dimensional nearest-neighbor asymmetric on-off models. A particularly interesting case is when the hopping bias is not parallel to any of the lattice directions. Fig. 9 displays the motion of the condensate in a  $20 \times 20$  square lattice with periodic boundary conditions where each

time a particle hops it either moves one site up or one site to the right with equal probabilities. The figure shows the  $x$ - and  $y$ -coordinates of the most occupied site and its occupation. It is intriguing to notice that the condensate moves alternatively up and to the right in quite an orderly fashion. Snapshots of the lattice (not presented here) reveal that the condensate typically consists of an L-shaped group of three highly occupied sites. At higher values of  $c$  the orderly motion is destroyed and the condensate drifts in the weak regime.

## 5. Exactly solvable non-Markovian ZRP

In this section we present a non-Markovian ZRP whose steady-state probability distribution factorizes into single site terms, similar to the usual Markovian ZRP. Thus, the steady-state distribution, the effective hopping rates and  $b_{\text{eff}}$  can be calculated exactly. A version of the model with totally asymmetric hopping is analyzed first in Sec. 5.1, and then the model and results are generalized to symmetric and partially asymmetric hopping in Sec. 5.2.

### 5.1. Totally asymmetric dynamics in 1-d

*5.1.1. Description of the model* The exactly solvable non-Markovian ZRP is a variant of the on-off model in which the advance of a clock of a site depends on the clock states of neighboring sites. Before presenting general results for partially-asymmetric hopping and for lattices in any dimensions, we begin for simplicity by considering a one-dimensional lattice with totally-asymmetric hopping.

The model is similar to the one described above in Sec. 2: at each site  $i$  of a one-dimensional lattice of  $L$  sites there are  $n_i$  particles, and a clock variable  $\tau_i = 0, 1$ , signifying “on” and “off”. Note that our notation here differs from that of Sec. 3.2, where  $\tau$  was allowed to take any integer value. This is not a significant difference, since, as discussed there, identifying all  $\tau \geq 1$  clock states with  $\tau = 1$  does not affect the dynamics. A particle can hop from site  $i$  to  $i + 1$  with rates (14), and once a particle jumps the clock at the target site is reset to zero. The only difference in the dynamics of the exactly solvable model is in the way the clocks are updated: the clock at site  $i$  can change from 0 to 1 only if  $\tau_{i+1} = 1$ . The allowed dynamical moves can be summarized as

$$\begin{aligned} \dots, (n_i, 1), (n_{i+1}, \tau_{i+1}), \dots &\xrightarrow{u(n_i)} \dots, (n_i - 1, 1), (n_{i+1} + 1, 0), \dots \\ \dots, (n_i, 0), (n_{i+1}, 1), \dots &\xrightarrow{c} \dots, (n_i, 1), (n_{i+1}, 1), \dots \end{aligned} \quad (35)$$

(here  $(n_i, \tau_i)$  signifies the occupation and clock state of site  $i$ ).

*5.1.2. The steady-state distribution* The goal of this section is to construct the steady state distribution of this model and show that it has a factorized form. Before doing so, we note that the factorized form is somewhat different from that presented in Eq. (4). The reason for the difference is that states in which all sites are off cannot be reached

by the dynamics of the model (all other states are possible). This introduces some correlations between the sites beyond those generated by the conservation of particles. The product measure which we discuss below is therefore of the form

$$\mathcal{P}(\mathbf{n}, \boldsymbol{\tau}) = Z_{L,N}^{-1} \prod_{i=1}^L f(n_i, \tau_i) \delta\left(\sum_{i=1}^L n_i - N\right) [1 - \delta(\boldsymbol{\tau})], \quad (36)$$

where  $\delta(\boldsymbol{\tau}) = 1$  if  $\boldsymbol{\tau} = 0$ , i.e., if all  $\tau_i = 0$ , and is zero otherwise. Here  $f(n, \tau)$  are the single-site weights. The normalization is accordingly given by

$$Z_{L,N} = \sum_{\mathbf{n}, \boldsymbol{\tau}} \prod_{i=1}^L f(n_i, \tau_i) \delta\left(\sum_{i=1}^L n_i - N\right) [1 - \delta(\boldsymbol{\tau})]. \quad (37)$$

In the thermodynamic limit, the weight of configurations with  $\boldsymbol{\tau} = 0$  becomes negligible, and therefore adding the square-brackets term in (36) and (37) does not affect this limit. We describe some properties of this factorized form in Appendix B. Note that the same product form also describes the finite-size product measure of the mean-field on-off model which was considered in Sec. 3.2.

The dynamics (35) defines an ergodic process (on the set of all configurations with a given number of particles and at least one ‘‘on’’ site), and therefore it has a unique steady state distribution. We now show that this distribution has a factorized form (36). This is done by assuming such a factorized form, and showing that it is indeed the unique stationary solution of the master equation. We begin by writing down the master equation. To this end we define a function  $W_{\tau_i, \tau_{i+1}}(n_i, n_{i+1})$  by

$$\begin{aligned} \mathcal{P}(\mathbf{n}, \boldsymbol{\tau}) W_{1,1}(n_i, n_{i+1}) &\equiv \mathcal{P}(\mathbf{n}, \{\dots, \tau_{i-1}, 0, 1, \dots\}) c - \mathcal{P}(\mathbf{n}, \boldsymbol{\tau}) u(n_i), \\ \mathcal{P}(\mathbf{n}, \boldsymbol{\tau}) W_{0,0}(n_i, n_{i+1}) &\equiv 0, \\ \mathcal{P}(\mathbf{n}, \boldsymbol{\tau}) W_{0,1}(n_i, n_{i+1}) &\equiv -\mathcal{P}(\mathbf{n}, \boldsymbol{\tau}) c, \\ \mathcal{P}(\mathbf{n}, \boldsymbol{\tau}) W_{1,0}(n_i, n_{i+1}) &\equiv -\mathcal{P}(\mathbf{n}, \boldsymbol{\tau}) u(n_i) + \sum_{\tau'=0,1} u(n_i + 1) \times \\ &\quad \mathcal{P}\left(\{\dots, n_i + 1, n_{i+1} - 1, \dots\}, \{\dots, \tau_{i-1}, 1, \tau', \tau_{i+2}, \dots\}\right). \end{aligned} \quad (38)$$

Note that  $W_{\tau_i, \tau_{i+1}}(n_i, n_{i+1})$  in fact depends on the full configuration  $(\mathbf{n}, \boldsymbol{\tau})$ . We suppress this dependence in the notation because if  $\mathcal{P}(\mathbf{n}, \boldsymbol{\tau})$  has a factorized form,  $W$  indeed depends only on the occupation and clock states of two adjacent sites (see Eq. (44) below).

Using the function  $W$ , the master equation can be written as

$$\dot{\mathcal{P}}(\mathbf{n}, \boldsymbol{\tau}) = \mathcal{P}(\mathbf{n}, \boldsymbol{\tau}) \sum_{i=1}^L W_{\tau_i, \tau_{i+1}}(n_i, n_{i+1}). \quad (39)$$

We elucidate Eqs. (38) and (39) through an example. Consider a configuration of a lattice of 4 sites with clocks  $\boldsymbol{\tau} = \{1, 1, 0, 0\}$  and some occupations  $\mathbf{n}$ . The different transitions into this configuration and out of this configuration can be enumerated one bond at a time:

- Sites 1 and 2: Since both clocks are on, the only possible transition involving both sites which would lead to this configuration is an advance of the clock at site 1, which occurs with rate  $c$ . The only possible transition out of this configuration which involves the two sites is a particle hopping from 1 to 2. Therefore, this bond contributes two terms to the master equation,

$$\mathcal{P}(\mathbf{n}, \{0, \tau_2, \dots\})c - \mathcal{P}(\mathbf{n}, \boldsymbol{\tau})u(n_1) = \mathcal{P}(\mathbf{n}, \boldsymbol{\tau})W_{1,1}(n_1, n_2). \quad (40)$$

- Sites 2 and 3: The first clock of the two is on while the second is off. The only possible transition involving these two sites leading to this configuration is a particle hopping from 2 to 3, and this is also the only possible transition out of this configuration. Therefore, this bond contributes to the master equation

$$\begin{aligned} \sum_{\tau_3=0,1} \mathcal{P}(\{\dots, n_2 + 1, n_3 - 1, \dots\}, \{\dots, 1, \tau_3, \dots\})u(n_2 + 1) - \mathcal{P}(\mathbf{n}, \boldsymbol{\tau})u(n_2) = \\ = \mathcal{P}(\mathbf{n}, \boldsymbol{\tau})W_{1,0}(n_2, n_3). \end{aligned} \quad (41)$$

- Sites 3 and 4: Both clocks are off, and therefore no transitions which involve only this bond are possible. One can define the contribution to the master equation as

$$0 = \mathcal{P}(\mathbf{n}, \boldsymbol{\tau})W_{0,0}(n_3, n_4). \quad (42)$$

- Sites 4 and 1: The first clock is off and the second is on. There are no transitions involving only this bond which can lead to this configuration. However, there is a possible transition out of this configuration, by an advance of the clock of site 4. The contribution from this bond is therefore

$$- \mathcal{P}(\mathbf{n}, \boldsymbol{\tau})c = \mathcal{P}(\mathbf{n}, \boldsymbol{\tau})W_{0,1}(n_4, n_1). \quad (43)$$

Summing up Eqs. (40)–(43) leads to the master equation (39). A similar analysis shows that the master equation has exactly the same form for any configuration and for any lattice size.

Now assume that  $\mathcal{P}(\mathbf{n}, \boldsymbol{\tau})$  has the factorized form (36). In this case, the definition (38) has the simpler form

$$\begin{aligned} W_{1,1}(n_i, n_{i+1}) &= \frac{f_{\text{off}}(n_i)}{f_{\text{on}}(n_i)}c - u(n_i), \\ W_{0,0}(n_i, n_{i+1}) &= 0, \\ W_{0,1}(n_i, n_{i+1}) &= -c, \\ W_{1,0}(n_i, n_{i+1}) &= \frac{f_{\text{on}}(n_i + 1)f(n_{i+1} - 1)}{f_{\text{on}}(n_i)f_{\text{off}}(n_{i+1})}u(n_i + 1) - u(n_i), \end{aligned} \quad (44)$$

where  $f_{\text{off}}(n) \equiv f(n, 0)$ ,  $f_{\text{on}}(n) \equiv f(n, 1)$ , and  $f(n) \equiv \sum_{\tau'} f(n, \tau')$ . In the steady state, the left-hand side of Eq. (39) vanishes and the equation becomes  $\sum_{i=1}^L W_{\tau_i, \tau_{i+1}}(n_i, n_{i+1}) = 0$ . This equation is solved by explicitly constructing its unique solution. This is done in two steps. First, we show that if one finds  $f(n, \tau)$  which satisfies

$$0 = W_{1,1}(n_i, n_{i+1}) \quad (45)$$

$$0 = W_{1,0}(n_i, n_{i+1}) + W_{0,1}(n_j, n_{j+1}) \quad (46)$$

for any  $n_i, n_{i+1}, n_j, n_{j+1}$ , this  $f$  is a solution to the equation. Then, we construct such an  $f$ .

The first step is achieved by noting that the number of  $W_{1,0}(n_i, n_{i+1})$  terms in the sum (39) exactly equals the number of  $W_{0,1}(n_j, n_{j+1})$  terms in the sum, since any configuration of  $\tau_i$ 's must have the same number of 01 and 10 nearest-neighbor pairs. Therefore, all terms in the sum (39) vanish either individually or in pairs, and the sum equals zero. We now construct a solution  $f$  which satisfies (45)–(46). Condition (45) is equivalent to

$$cf_{\text{off}}(n) = u(n)f_{\text{on}}(n). \quad (47)$$

For condition (46), note that  $W_{0,1}(n_j, n_{j+1})$  is in fact independent of  $n_j, n_{j+1}$  (see Eq. (44)). Therefore, this condition together with (47) yield

$$\frac{f(n_i + 1)}{f(n_i)} \frac{u(n_i + 1)}{c + u(n_i + 1)} = \frac{f(n_{i+1})}{f(n_{i+1} - 1)} \frac{u(n_{i+1})}{c + u(n_{i+1})}, \quad (48)$$

As the occupations  $n_i$  and  $n_{i+1}$  may vary independently, this equation holds only if both sides are equal to a constant, which might be set to  $1/c$  without loss of generality (as it only affects the normalization constant  $Z_{L,N}$ ). We therefore find that

$$f(n)\bar{u}(n) = f(n - 1) \quad (49)$$

where

$$\frac{1}{\bar{u}(n)} = \frac{1}{c} + \frac{1}{u(n)}, \quad (50)$$

compare with equations (9) and (20). Choosing the constant to be  $1/c$  guarantees that, as we show below,  $\bar{u}(n)$  as defined in Eq. (50) are the effective hopping rates.

The conclusion from Eqs. (47)–(50) is that the factorized probability distribution of the form (36) with

$$f(n, 1) \equiv f_{\text{on}}(n) = \frac{c}{c + u(n)} f(n), \quad (51)$$

$$f(n, 0) \equiv f_{\text{off}}(n) = \frac{u(n)}{c + u(n)} f(n), \quad (52)$$

$$f(n) = \prod_{k=1}^n \frac{1}{\bar{u}(k)} = \prod_{k=1}^n \left[ \frac{1}{c} + \frac{1}{u(k)} \right]. \quad (53)$$

is the stationary solution of model. It is easy to verify using (50) and (51) that  $\bar{u}(n) = \frac{f_{\text{on}}(n)u(n)}{f(n)}$ , and therefore  $\bar{u}(n)$  are the effective hopping rates as defined in Eq. (10).

Using the results (51)–(53), one can calculate numerically the stationary probability for any configuration in a finite system of size  $L$  with  $N$  particles (recursion relations that facilitate this calculation are presented in Appendix B). Condensation in the model is determined by the probability measure in the thermodynamic limit. The factorized product measure (36) and Eq. (49) imply that this model has the same thermodynamic behavior as a Markovian ZRP with effective hopping rates (50) (see Appendix B). One

can thus study condensation in the model using known properties of the ZRP, as was done in Sec. 3. In particular, for rates of the form  $u(n) = 1 + b/n + O(n^{-2})$ , one finds

$$\bar{u}(n) = \frac{c}{1+c} \frac{1 + \frac{b}{n} + O(n^{-2})}{1 + \frac{b}{(1+c)n} + O(n^{-2})} = J_c \left[ 1 + \frac{b_{\text{eff}}}{n} + O(n^{-2}) \right] \quad (54)$$

with

$$J_c = \frac{c}{1+c} < 1 \quad \text{and} \quad b_{\text{eff}} = J_c b < b. \quad (55)$$

Here,  $J_c$  is the current at the critical density, and  $b_{\text{eff}}$  is the parameter controlling condensation. In other words, condensation may occur only when  $b_{\text{eff}} > 2$ , or  $b > 2/J_c$  (compare with the MF values in Eqs. (21)–(24), and note also that at criticality, the probability to find a site in the off state is  $P_{\text{off}} = J_c/c$ , rather than (17) of the MF model).

## 5.2. Partially asymmetric dynamics and higher-dimensional lattices

*5.2.1. Description of the model* The exactly solvable model described above can still be fully analyzed when the dynamics is generalized to partially asymmetric or symmetric dynamics and to certain higher dimensional lattices. Moreover, the stationary distribution turns out to be independent on the asymmetry or the dimension. We described the generalized dynamics and its solution in this section.

First, consider dynamics on a 1-d lattice that allows for partially asymmetric hopping. This is implemented as discussed above in Eq. (3): when a particle jumps from an “on” site  $i$  (an event which occurs with a rate  $u(n)$ ), it randomly chooses its target site: with probability  $1 - p$  it moves to site  $i + 1$  and otherwise (i.e. with probability  $p$ ) it moves to  $i - 1$ . Here  $0 \leq p \leq 1$  is the asymmetry parameter:  $p = 1/2$  corresponds to symmetric dynamics, while  $p = 0$  corresponds to a totally asymmetric bias to the right.

For the stationary distribution to factorize, one must also modify the update rule for the clock variable, in the following manner. At each “off” site, an attempt to update the clock is made with rate  $c$ . Once an attempt is made at, say, site  $i$ , a neighboring site is chosen at random with the *same* asymmetry parameter  $p$ : site  $i + 1$  is chosen with probability  $1 - p$  and site  $i - 1$  with probability  $p$ . Finally, if the chosen site is in an “on” state, the clock of site  $i$  is turned on. The generalized dynamics can be summarized as

$$\begin{aligned} \dots, (n_i, 1), (n_{i+1}, \tau_{i+1}), \dots &\xrightarrow{(1-p)u(n_i)} \dots, (n_i - 1, 1), (n_{i+1} + 1, 0), \dots \\ \dots, (n_{i-1}, \tau_{i-1}), (n_i, 1), \dots &\xrightarrow{pu(n_i)} \dots, (n_{i-1} + 1, 0), (n_i - 1, 1), \dots \\ \dots, (n_i, 0), (n_{i+1}, 1), \dots &\xrightarrow{(1-p)c} \dots, (n_i, 1), (n_{i+1}, 1), \dots \\ \dots, (n_{i-1}, 1), (n_i, 0), \dots &\xrightarrow{pc} \dots, (n_{i-1}, 1), (n_i, 1), \dots, \end{aligned} \quad (56)$$

where the first line describes a particle jump from  $i$  to the right, the second describes a jump to the left, and the third and fourth lines describe the two update processes of the clock at site  $i$ .



In a similar fashion, the model can be generalized to symmetric or biased dynamics on higher dimensional lattices. Here we consider for concreteness cubic lattices in  $d$ -dimensions, although the argument which we present below for the factorization of the stationary distribution is valid for other lattices, e.g. a triangular lattice in  $2d$ .<sup>‡</sup> As in the partially asymmetric case, a particle leaves any site  $i$ , if it is on, with rate  $u(n)$ . It then selects its target from among the  $2d$  nearest neighbors of  $i$  according to an asymmetry probability vector  $p_a$ , where  $a = 1, \dots, 2d$  denotes the direction (for example, in two dimensions  $a = 1, 2, 3, 4$  could correspond to north, east, south and west) and  $\sum_{a=1}^{2d} p_a = 1$ . A choice of  $p_a = 1/2d$  for all  $a$  corresponds to symmetric dynamics, and any other choice would result in biased hopping. The clock update rule in the  $d$ -dimensional case is similarly generalized: if site  $i$  is off, an attempt to update its clock is made with rate  $c$ . At each attempt, the neighbor of  $i$  in the direction  $a$  is chosen with probability  $p_a$ , and if the chosen neighbor is on the clock of  $i$  is updated.

Since 1-dimensional partially asymmetric hopping is a particular case of  $d$ -dimensional dynamics, both cases are treated below together.

*5.2.2. The steady-state distribution* The factorization in the generalized case is demonstrated as done above, by explicitly constructing the stationary measure. To this end it is once again assumed that the stationary measure has the factorized form (36)–(37). The master equation for this factorized distribution reads, at the steady state,

$$0 = \dot{\mathcal{P}}(\mathbf{n}, \boldsymbol{\tau}) = \mathcal{P}(\mathbf{n}, \boldsymbol{\tau}) \sum_{a=1}^{2d} p_a \left[ \sum_{i=1}^L W_{\tau_i, \tau_{i+a}}(n_i, n_{i+a}) \right], \quad (57)$$

where site  $i + a$  denotes the neighbor of site  $i$  in the direction  $a$ , and  $W$  is defined in (44).

The key observation which facilitates finding a solution to this master equation is that for each  $i$  and  $a$  such that  $\tau_i = 1$  and  $\tau_{i+a} = 0$ , there exists exactly one site  $j$  whose clock is  $\tau_j = 0$  while  $\tau_{j+a} = 1$ . This can be seen for example by examining the clocks of all sites on the ray which starts at site  $i$  and is in direction  $a$  (i.e., by examining sites  $i + 2a, i + 3a, \dots$ ), which leads to a situation similar to the one-dimensional case. Therefore, a solution to Eq. (57) can be found if  $W_{1,1}(n, n') = 0$  and  $W_{1,0}(n, n') + W_{0,1} = 0$  for all  $n$  and  $n'$  (note again that  $W_{0,1} \equiv W_{0,1}(n, n')$  is independent of  $n, n'$ ). These are precisely the conditions which appeared in the totally asymmetric case, and therefore they are fulfilled by the same solution — Eqs. (51)–(53).

We have thus shown that the stationary distribution of the generalized model factorizes, and moreover it is independent of asymmetry and lattice dimension. In particular, condensation is independent of the asymmetry parameter, and the results of Sec. 5.1.2 apply.

<sup>‡</sup> Note, however, that the argument does not hold for *all* higher dimensional lattices. For example, the argument fails for a  $2d$  honeycomb lattice.

## 6. Conclusions

The analysis presented above reveals that non-Markovian dynamics may have two major effects on the condensation transition of the ZRP. First, the parameter  $b$  which controls condensation is “renormalized” by the existence of memory in the dynamics, and thus a memory may suppress or induce condensation. For models with mean-field dynamics and for an exactly solvable variant of the model, the effective rates could be computed exactly, and thus the modified criterion for condensation was found. Numerically, the condensation in models with nearest-neighbor hopping were also found to be controlled by an effective  $b$ , although one which differs from the mean-field value. Calculating the effective hopping rates in nearest-neighbor models remains an open problem which may be of practical importance when one wishes to use a non-Markovian ZRP to study condensation in other systems.

A second effect of the memory is perhaps more dramatic: the condensate is found to move from one site to the next when the dynamics is of asymmetric nearest-neighbor hopping. Numerical studies of finite systems identify two modes of condensate drift: a strong-drift regime with continuous “slinky” motion and a weak-drift regime in which the motion is more erratic. Both modes of motion are rather robust to changes in the dynamics. The behavior of the model in the thermodynamic limit is not yet known, and it would be interesting to ascertain whether there is a sharp transition between them, or, if such a transition does not exist, to understand the crossover from one regime to the other.

The mechanism which leads to the condensate drift is understood on a heuristic level and is expected to be a generic feature of many systems which undergo a condensation transition and which are asymmetric and have some spatial correlations [17]. However, a more quantitative understanding of this drift, for example the calculation of the drift velocity, remains an important open problem. It is also interesting to explore similar effects in other mass-transport systems, such as driven diffusive systems and shaken granular gases. In this respect, it should be noted that a mass-transport model with a moving condensate was recently identified in [22]. There, a variant of the ZRP is studied which has a factorized steady-state and in which unbound hopping rates lead to a condensate which reaches an infinite velocity. A product measure steady state with a moving condensate is not possible in systems with finite hopping rates like ours.

We have also studied an exactly soluble variant of the non-Markovian model with nearest-neighbor hopping whose steady state factorizes. In this variant, as in the mean-field model, condensation is controlled by an effective  $b$  and no condensate motion appears. It should be noted that although the model has a product measure, particle currents are temporally correlated.

## Acknowledgments

The support of the Israel Science Foundation (ISF) is gratefully acknowledged.

## Appendix A. Regular and irregular clocks

As stressed above, the internal clock variables  $\tau_i$  do not measure an exact time, but rather proceed in an irregular stochastic fashion. In this Appendix, it is shown that regular clock, that proceed in a deterministic continuous fashion, may be obtained from the dynamical rules (1) by taking an appropriate limit.

We denote the clock variables in this Appendix as  $m_i$  instead of  $\tau_i$ , to emphasized that they may attain only integer values. In order to obtain regular clocks, define new clock variables  $\tau_i = m_i d\tau$ , where  $d\tau$  is an infinitesimal time unit which will eventually be taken to zero. The new clock variables are no longer integer: they can attain any value  $\tau = 0, d\tau, 2d\tau, 3d\tau, \dots$ , and in the limit of infinitesimal  $d\tau$  they become continuous variables. In addition, the rate with which  $m_i$  advances to  $m_i + 1$  is taken as  $c = 1/d\tau$ . Finally, the hopping rates out of each site  $i$  are taken to depend on  $\tau_i$  rather than  $m_i$ , and thus they can be written as  $u(n_i, \tau_i)$ . The limit of regular clocks is then obtained by taking the limit  $d\tau \rightarrow 0$ , while keeping  $\tau_i$  fixed.

For example, consider an on-off model with regular clocks, whose hopping rates are  $u(n, \tau) = u(n)\Theta(\tau/\tau_0 - 1)$ , where  $\tau_0$  is a constant and  $\Theta(x)$  is the Heaviside theta function. Such a model may be achieved by considering irregular-clock models (1) with rates  $u(n, m) = u(n)\Theta(m d\tau/\tau_0 - 1)$  and  $c = 1/d\tau$ , and taking the limit  $d\tau \rightarrow 0$  while keeping the constant  $\tau_0$  fixed. In this regular-clock on-off model, whenever a particle hops into a site this site is turned off for a duration of exactly  $\tau_0$  time units. The solution of such a model with mean-field dynamics may be found from an analysis similar to that presented in Sec. 3 [23]. Similarly, more general regular-clock models with rates  $u(n, \tau) = u(n)v(\tau)$  can be obtained by taking the limit of irregular-clock models with rates  $u(n, m) = u(n)v(m d\tau/\tau_0)$  (the function  $v$  remains unchanged when taking the limit).

## Appendix B. Properties of factorized distributions of the form (36)

In this Appendix we present some of the properties of the stationary distribution of the exactly solvable on-off model, which has the factorized form (36) with partition function (37). The goal of this Appendix is to present recursion relations which allow the calculation of this product measure for any finite system size, and to demonstrate that such product measures lead to the same thermodynamic behavior as (4) and (5).

We begin by defining two auxiliary partition sums,

$$\bar{Z}_{L,N} = \sum_{\mathbf{n}, \boldsymbol{\tau}} \prod_{i=1}^L f(n_i, \tau_i) \delta\left(\sum_{i=1}^L n_i - N\right), \quad (\text{B.1})$$

$$Z_{L,N}^{\text{off}} = \sum_{\mathbf{n}} \prod_{i=1}^L f_0(n_i) \delta\left(\sum_{i=1}^L n_i - N\right), \quad (\text{B.2})$$

and two auxiliary distributions,

$$\bar{\mathcal{P}}(\mathbf{n}, \boldsymbol{\tau}) = \frac{1}{\bar{Z}_{L,N}} \prod_{i=1}^L f(n_i, \tau_i) \delta\left(\sum_{i=1}^L n_i - N\right), \quad (\text{B.3})$$

$$\mathcal{P}^{\text{off}}(\mathbf{n}) = \frac{1}{Z_{L,N}^{\text{off}}} \prod_{i=1}^L f_0(n_i) \delta\left(\sum_{i=1}^L n_i - N\right). \quad (\text{B.4})$$

Here and in the rest of this section we denote  $f_0(n) \equiv f(n, 0)$  and  $f_1(n) \equiv f(n, 1)$ . This is done to avoid confusion with the superscript “off”, which will be used below to denote quantities calculated using the distribution (B.4). As before, we denote  $f(n) \equiv f_0(n) + f_1(n)$ , and we adopt the convention of Sec. 5 whereby the clocks may have only two values,  $\tau = 0, 1$ .

Using these notations and the definition (37) one immediately finds that

$$Z_{L,N} = \bar{Z}_{L,N} - Z_{L,N}^{\text{off}}. \quad (\text{B.5})$$

We first analyze the auxiliary distributions before treating the original problem. By summing over the occupations and clock states of all sites but one, the probability to find a single site in any given state is found to be

$$\begin{aligned} \bar{P}(n, \tau) &\equiv \sum_{\substack{n_2, \dots, n_L \\ \tau_2, \dots, \tau_L}} \bar{\mathcal{P}}(n, n_2, \dots, n_L; \tau, \tau_2, \dots, \tau_L) \delta\left(\sum_{i=2}^L n_i - (N - n)\right) = \\ &= f(n, \tau) \frac{\bar{Z}_{L-1, N-n}}{\bar{Z}_{L,N}}, \end{aligned} \quad (\text{B.6})$$

$$P^{\text{off}}(n) \equiv \sum_{n_2, \dots, n_L} \mathcal{P}^{\text{off}}(n, n_2, \dots, n_L) \delta\left(\sum_{i=2}^L n_i - (N - n)\right) = f_0(n) \frac{Z_{L-1, N-n}^{\text{off}}}{Z_{L,N}^{\text{off}}}. \quad (\text{B.7})$$

Summing both equations over  $n$  leads to the recursion relations

$$\bar{Z}_{L,N} = \sum_{n=0}^N \bar{Z}_{L-1, N-n} f(n), \quad (\text{B.8})$$

$$Z_{L,N}^{\text{off}} = \sum_{n=0}^N Z_{L-1, N-n}^{\text{off}} f_0(n). \quad (\text{B.9})$$

When  $f(n, \tau)$  are known, these recursion formulas can be used for a numerical calculation of the auxiliary partition sums, and thus, using (B.5) also of  $Z_{L,N}$ .

Knowing the partition function  $Z_{L,N}$ , other quantities of interest can be computed. For example, repeating the calculation of (B.6) for the original product measure yields

$$P(n, \tau) = f(n, \tau) \frac{Z_{L-1, N-n} + \delta_{\tau,1} Z_{L-1, N-n}^{\text{off}}}{Z_{L,N}}, \quad (\text{B.10})$$

where  $\delta_{\tau,1}$  is the Kronecker delta. The current can be found in a similar fashion by calculating

$$\langle u(n) \rangle \equiv \sum_{n=1}^N P(n, 1) u(n) = \sum_{n=1}^N f(n, 1) u(n) \frac{\bar{Z}_{L-1, N-n}}{Z_{L,N}} = \sum_{n=0}^{N-1} f(n) \frac{\bar{Z}_{L-1, N-1-n}}{Z_{L,N}}$$

$$= \frac{\bar{Z}_{L,N-1}}{Z_{L,N}}, \quad (\text{B.11})$$

where (51)–(53) were used to deduce that  $f(n,1)u(n) = f(n-1)$ , and we have used (B.5) and (B.10).

In the thermodynamic limit, the partition function can be analyzed by transforming to the grand-canonical ensemble. Mathematically this is done by introducing the grand-canonical partition function which is the generating function

$$\mathcal{Z}_L(z) \equiv \sum_{N=0}^{\infty} z^N Z_{L,N}. \quad (\text{B.12})$$

Using the definition (37), one can split the sum into two contributions,  $\mathcal{Z}_L(z) = \bar{\mathcal{Z}}_L - \mathcal{Z}_L^{\text{off}}$ , where

$$\bar{\mathcal{Z}}_L \equiv \sum_{N=0}^{\infty} z^N \bar{Z}_{L,N} = \bar{F}(z)^L, \quad \mathcal{Z}_L^{\text{off}} \equiv \sum_{N=0}^{\infty} z^N Z_{L,N}^{\text{off}} = F^{\text{off}}(z)^L, \quad (\text{B.13})$$

and

$$\bar{F}(z) \equiv \sum_{n=0}^{\infty} f(n)z^n, \quad F^{\text{off}}(z) \equiv \sum_{n=0}^{\infty} f_0(n)z^n. \quad (\text{B.14})$$

Using (51)–(53), one has  $F^{\text{off}}(z) = z\bar{F}(z)/c$ , from which the grand-canonical partition function is found to be

$$\mathcal{Z}_L(z) = \bar{\mathcal{Z}}_L(z) \left[ 1 - \left( \frac{z}{c} \right)^L \right]. \quad (\text{B.15})$$

If the radius of convergence of the sum (B.12), or equivalently of (B.14), is smaller than  $c$ , then the correction due to the weak correlation between clocks is exponentially small when  $L$  is large. For hopping rates of the form  $u(n) \simeq 1 + b/n$ , this radius of convergence is  $z_c = c/(1+c) < c$  (see Eq. (53)), and therefore, in this case  $(z/c)^L$  is indeed negligible. Note that  $z_c$  is the current  $J_c$  of the canonical system at the condensation transition, Eq. (55).

The relation between the fugacity  $z$  and the canonical density  $\rho$  is given by

$$\rho = \frac{z}{L} \frac{\partial \log \mathcal{Z}(z)}{\partial z} = z \frac{\bar{F}'(z)}{\bar{F}(z)} + \frac{1}{1 - (z/c)^L}, \quad (\text{B.16})$$

which is an implicit equation for  $z(\rho)$ . This is the same expression as that of a Markovian ZRP with rates  $\bar{u}(n)$ , up to a correction which is exponentially small in  $L$ .

## References

- [1] M. R. Evans and T. Hanney. Nonequilibrium statistical mechanics of the zero-range process and related models. *J. Phys. A*, 38:R195–R240, May 2005.
- [2] S. N. Majumdar. Real-space Condensation in Stochastic Mass Transport Models. In J. Jacobsen et al., editors, *Exact Methods in Low-Dimensional Statistical Physics and Quantum Computing: Lecture Notes of the Les Houches Summer School July 2008*, volume 89. Oxford University Press, Oxford, 2010.

- [3] A. Schadschneider, D. Chowdhury, and K. Nishinari. *Stochastic Transport in Complex Systems: From Molecules to Vehicles*. Elsevier Science, Amsterdam, 2010.
- [4] K. van der Weele, D. van der Meer, M. Versluis, and D. Lohse. Hysteretic clustering in granular gas. *Europhys. Lett.*, 53:328–334, February 2001.
- [5] S. N. Dorogovtsev and J. F. F. Mendes. *Evolution of Networks*. Oxford University Press, Oxford, 2003.
- [6] Z. Burda, D. Johnston, J. Jurkiewicz, M. Kamiński, M. A. Nowak, G. Papp, and I. Zahed. Wealth condensation in pareto macroeconomies. *Phys. Rev. E*, 65(2):026102, February 2002.
- [7] J. Kaupužs, R. Mahnke, and R. J. Harris. Zero-range model of traffic flow. *Phys. Rev. E*, 72(5):056125, November 2005.
- [8] M. R. Evans. Phase Transitions in One-Dimensional Nonequilibrium Systems. *Brazilian Journal of Physics*, 30:42–57, March 2000.
- [9] Y. Kafri, E. Levine, D. Mukamel, G. M. Schütz, and J. Török. Criterion for Phase Separation in One-Dimensional Driven Systems. *Phys. Rev. Lett.*, 89(3):035702, June 2002.
- [10] E. Levine, D. Mukamel, and G. M. Schütz. Long-range attraction between probe particles mediated by a driven fluid. *Europhys. Lett.*, 70:565–571, June 2005.
- [11] A. Rákos, E. Levine, D. Mukamel, and G. M. Schütz. Dynamical scaling for probe particles in a driven fluid. *J. Stat. Mech.: Theory Exp.*, 11:1, November 2006.
- [12] S. Chatterjee and M. Barma. Dynamics of shock probes in driven diffusive systems. *J. Stat. Mech.: Theory Exp.*, 1:4, January 2007.
- [13] S. Chatterjee and M. Barma. Shock probes in a one-dimensional Katz-Lebowitz-Spohn model. *Phys. Rev. E*, 77(6):061124, 2008.
- [14] O. Hirschberg, D. Mukamel, and G. M. Schütz. Condensation in Temporally Correlated Zero-Range Dynamics. *Phys. Rev. Lett.*, 103(9):090602, August 2009.
- [15] E. D. Andjel. Invariant measures for the zero range process. *Ann. Prob.*, 10(3):525–547, 1982.
- [16] M. R. Evans, S. N. Majumdar, and R. K. P. Zia. Canonical Analysis of Condensation in Factorised Steady States. *J. Stat. Phys.*, 123:357–390, April 2006.
- [17] O. Hirschberg, D. Mukamel, and G. M. Schütz. in preparation.
- [18] S. Grosskinsky, G. M. Schütz, and H. Spohn. Condensation in the zero range process: stationary and dynamical properties. *J. Stat. Phys.*, 113:389–410, November 2003.
- [19] C. Godrèche and J. M. Luck. Dynamics of the condensate in zero-range processes. *J. Phys. A*, 38:7215–7237, August 2005.
- [20] J. Beltrán and C. Landim. Metastability of reversible condensed zero range processes on a finite set. *Probability Theory and Related Fields*, 152:781–807, 2012.

- [21] C. Landim. Metastability for a non-reversible dynamics: the evolution of the condensate in totally asymmetric zero range processes. *Arxiv preprint arXiv:1204.5987*, 2012.
- [22] B. Waclaw and M. R. Evans. Explosive Condensation in a Mass Transport Model. *Phys. Rev. Lett.*, 108(7):070601, February 2012.
- [23] O. Hirschberg. Condensation in non-equilibrium systems with non-Markovian dynamics. Master's thesis, Weizmann Institute of Science, Israel, 2009.